Chin. Geogra. Sci. 2022 Vol. 32 No. 3 pp. 537−548
https://doi.org/10.1007/s11769-022-1282-4

Springer Science Press
www.springerlink.com/content/1002-0063

Geochemistry of Sediments from a Subalpine Lake Sedimentary Succession in the Western Nanling Mountains, Southern China: Implications for Catchment Weathering During the Last 15 400 Years

WANG Bingxiang[1], ZHONG Wei[1], ZHU Chan[2], OUYANG Jun[1], WEI Zhiqiang[3], SHANG Shengtan[4]

(1. *School of Geography Sciences*, *South China Normal University*, *Guangzhou* 510631, *China*; 2. *Guangdong Center for Marine Development Research*, *Guangzhou* 510220, *China*; 3. *Zhuhai Branch of State Key Laboratory of Earth Surface Processes and Resource Ecology*, *Faculty of Geographical Science*, *Beijing Normal University*, *Zhuhai*, *Guangdong* 519087, *China*; 4. *School of Earth Science and Engineering*, *Sun Yat-sen University*, *Zhuhai* 519082, *China*)

Abstract: In the present work, 15 400 yr old geochemical records of a core from the subalpine Daping swamp are presented with the aim to examine the relationship between the chemical weathering and the climatic changes in the region of the western Nanling Mountains, China. The climate of the study region was deeply controlled by the East Asian summer monsoon. The results indicate that, in the past 15 400 yrs, the values of chemical index of alteration (CIA) ranged from 73.9% to 88.2% (mean: 85.3%), suggested a medium and high intensity of chemical weathering. The local exogenous clastic materials, which were derived from the weathered residues, played a key role in contributing towards the sediments. Since the climate-induced chemical weathering exerted strong influences on the geochemical features of weathered residues, the geochemical characteristics of the sediments were deeply impacted by climatic conditions. Wetter and warmer conditions would favor increased chemical weathering, resulting in more leaching of soluble and mobile elements (e.g., Ba and Sr) and leaving the resistant and immobile elements (e.g., Al and Ti) enriched in the weathered residues. These materials were then eroded and transported into the lake, and led to the sediments characterized by the characteristic of having depleted soluble elements. In contrast, dry and cold conditions would result in an opposite trend. In this sense, the geochemical records can serve as proxies to indicate changes of chemical weathering intensity, which were closely related to the evolution of summer monsoon.

Keywords: lacustrine sediments; chemical weathering; asian summer monsoon; last deglacial; western Nanling Mountains; China

Citation: WANG Bingxiang, ZHONG Wei, ZHU Chan, OUYANG Jun, WEI Zhiqiang, SHANG Shengtan, 2022. Geochemistry of Sediments from a Subalpine Lake Sedimentary Succession in the Western Nanling Mountains, Southern China: Implications for Catchment Weathering During the Last 15 400 Years. *Chinese Geographical Science*, 32(3): 537−548. https://doi.org/10.1007/s11769-022-1282-4

1 Introduction

Chemical weathering is an important supergene geochemical behavior of the interaction among various layers of the earth's surface. The processes of the migration and transformation of weathering products record the changes of paleoenvironment. Therefore, chemical weathering is also an important means of the inversion of past climate change (Jin et al., 2001a; 2006; Li and Yang, 2010; Hartmann and Moosdorf, 2011). The denudation and chemical weathering of silicate rocks can affect the global climate by affecting the global carbon cycle. A number of studies have demonstrated that the weathering rates in soils and small catchments have

Received date: 2021-05-06; accepted date: 2021-08-01
Foundation item: Under the auspices of the National Natural Science Foundation of China (No. 41971101, 41571187, 41071137)
Corresponding author: ZHONG Wei. E-mail: zhongwei@m.scnu.edu.cn

been found to be linked with significant climate effect (White and Blum, 1995; White and Brantley, 2003; Miriyala et al., 2017). Recent studies have demonstrated that increased chemical weathering can rapidly respond to climatic changes (Degeai et al., 2018; Wang et al., 2020; Liu et al., 2021). Even in high-latitude places, such as Iceland, it is estimated that climatic change over the past four decades resulted in up to 30% increase in the chemical weathering flux (Gislason et al., 2009). A more recent study concerning the responses of chemical weathering to deglacial-to-mid-Holocene summer monsoon intensification in the Myanmar watersheds reveals that the weathering was not a later amplifier, but worked in tandem with global climate change, which was closely related to the changes in monsoonal temperature and humidity (Miriyala et al., 2017).

The typical Asian summer monsoon (ASM) influenced regions, where involve obvious temperature and humidity changes both critical for intensive chemical weathering, and whether the climatic changes have triggered the erosion and weathering, are ideal places to assess the linkage between climatic changes and chemical weathering. In this sense, the Nanling Mountains (NLM) (24°00′N–29°00′N, 110°00′E–120°00′E, ~1500–2000 m a.s.l. (above sea level)) is an ideal region to study this issue because it is located in the core of the tropical monsoon regions (Gao et al., 1962), confronting East Asian summer monsoon (EASM) and functioning as the last barrier to winter monsoon in southern China. The western part of the NLM is located in the transitional belt between the EASM and the Indian summer monsoon (ISM) systems (Qian et al., 2007), specific geographical location makes this region particularly sensitive to shifts in monsoon rainfall patterns. A detailed investigation on the relationship between the chemical weathering and the climatic changes would provide new insights into the evolution of the ASM. A large number of studies have demonstrated that the concentration of major and trace elements in lake sediments are sensitive to temperature/precipitation changes (Gislason et al., 2009; Boës et al., 2011; Liu et al., 2020; Li et al., 2021), which can provide useful information on elucidating the relationship between the chemical weathering and the climatic changes.

Based on a well-dated sedimentary core from Daping swamp in western NLM, the present study emphasizes temporal variation characteristics of element content, including Al_2O_3, TiO_2, MnO, FeOt, Rb, Sr, Cu and Ba, and ratios (Rb/Sr, SiO_2/Al_2O_3, MnO/Al_2O_3 and $FeOt/Al_2O_3$), as well as chemical index of alteration (CIA). The CIA results, integrated with dry bulk density, organic carbon isotope, pollen and grain size, reveal the paleoenvironmental/paleoclimatic evolution and the chemical weathering history of the Daping swamp since the Last Deglaciation. The purpose of this study was highlight importance of regional chemical weathering in interpreting the past climatic changes, which were related to the ASM.

2 Study Site

Daping swamp (26°10′11″N–26°10′42″N, 110°07′25″E–110°08′00″E) is situated in the Daping Basin, located in the weatern NLM in South China, is important geographic division of the middle and southern subtropical zones (Fig. 1). Previous studies revealed that the sedimentary succession from the Daping swamp, which was developed in the closed subalpine intermontane basin, was an ideal geologic achieve for reconstructing the climatic and environmental changes (Zhong et al., 2015a; 2017). Field investigations revealed that the bedrocks in the study region are dominated by medium-grained porphyritic granites in the early Yanshan stage in the Mesozoic period, whereas the main minerals are potash feldspar, plagioclase, quartz and biotite (Zhu et al., 2009; Wang et al., 2013). The mean temperature in January and July are –0.5°C and 19°C respectively, with a mean annual temperature of ~ 10.9°C. Mean annual precipitation is about 2000 mm, and the annual evaporation is ~ 500 mm. The regional vegetation is dominated by subtropical evergreen broad-leaved forest and deciduous broad-leaved forest (Wu, 1980; Zhong et al., 2015b).

3 Materials and Methods

A 236-cm-long core (designated core DP-2011-02), which was extracted in Sept. 2011 using a piston coring device produced by Christie Engineering (Australia) (CHPD 52), was used for this study. In the field, this core was cut lengthwise, photographed and described. Samples were then transported to the laboratory and stored at 4°C.

Eight organic-rich bulk sample cores (laboratory code LUG11-*n*) (Table 1) were collected from the study site

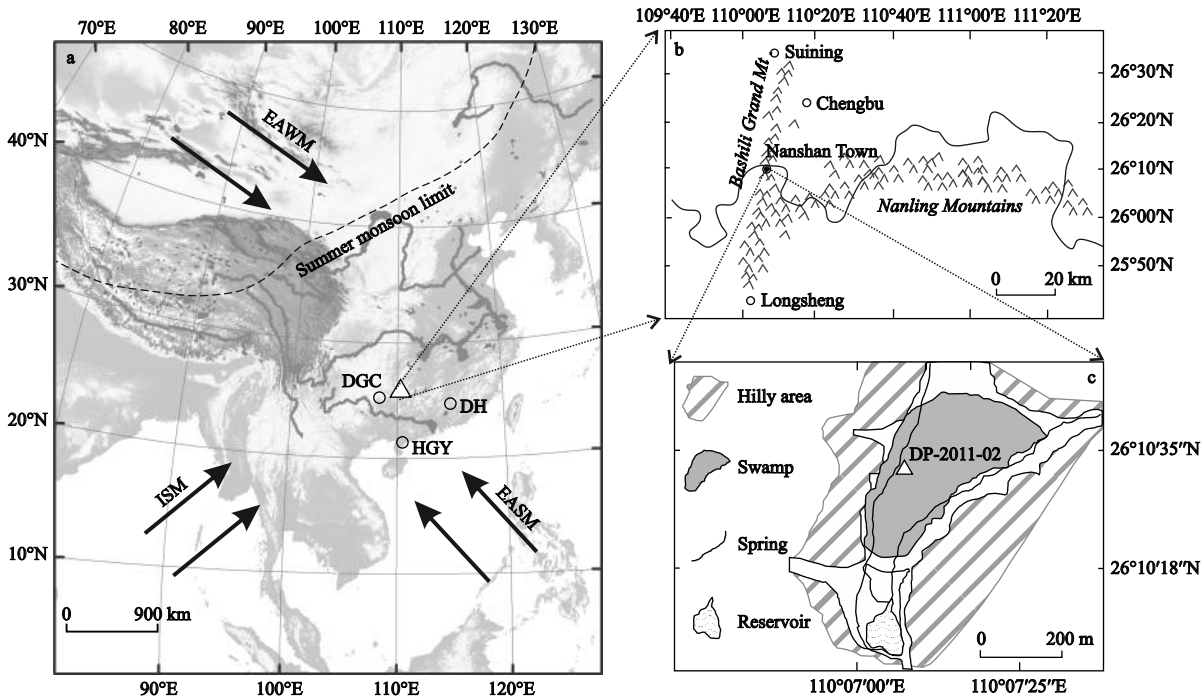

Fig. 1 Climate background, geographic location and profile of Daping area. a. the climatic system of China including the East Asian summer monsoon (EASM) and Indian summer monsoon (ISM); the East Asian winter monsoon (EAWM) winds associated with the Siberian-Mongolian High and the Westerly winds generalized as the mean locations of jet stream are indicated; the comparison sites are Dahu swamp (DH) (Wang et al., 2021), Dongge cave (DGC) (Dykoski et al., 2005) and Huguangyan Maar lake (HGY) (Wang et al., 2016), and the latitude position is similar to the Daping swamp, which is considered to be affected by EASM and ISM. b. the location of study region; c. the location of the study core (Modified after Zhong et al., 2015a)

Table 1 Radiocarbon dating results using the Intcal 20 calibration dataset for the core DP-2011-02 in Daping swamp

Lab. code	Depth /cm	Material	Age / ^{14}C yr B.P.	Calibrated age	
				cal. yr B.P. (2 sigma)	Intercept (cal. yr B.P.)
LUG11-198	24−29	TOC	673 ± 87	542−1073	720
LUG11-199	54−59	TOC	2218 ± 113	2010−2786	2380
LUG11-200	67−72	TOC	3768 ± 94	3573−4303	3980
LUG11-201	81−86	TOC	4119 ± 95	4403−4969	4674
LUG11-202	108−113	TOC	5428 ± 158	5846−6773	6270
LUG11-204B1	151−156	TOC	8895 ± 128	9880−11132	10460
LUG11-205	183−188	TOC	11373 ± 127	12540−13444	13120
LUG11-206	223−228	TOC	12452 ± 167	14187−15409	14780

Notes：TOC, total organic carbon in lake sediments

for conventional radiocarbon dating using liquid scintillation technique at the Key Laboratory of Western China's Environmental Systems (Ministry of Education of China) at the Lanzhou University, China. The specific method was detailed described in Zhong et al. (2015a). In this study, the radiocarbon ages were re-calibrated using the latest IntCal 20 calibration datasets (Reimer et al., 2020). A linear interpolation method (Yeloff et al., 2006; Machlus et al., 2015) was used to establish the core chronological sequence based on the mean sedimentation rates of the two adjacent calibration ages.

Samples were collected at 2-cm intervals for chemical element analysis. All samples were freeze-dried and ground using ZHM-1A vibration grinding prototype (Beijing Zhonghe Chuangye, China). After grinding, the

particle size of the samples was < 74 μm. First, 6.0 g of powdered samples were taken and boric acid was used as the sides and bottom. The samples were then pressed into a round cake with a diameter of 3.2 cm and analyzed for the contents of major and trace elements using the polarization energy dispersive X-ray fluorescence spectrometer (Epsilon 5) procured from PANalytical B.V., The Netherlands. The analytical error in the contents of elements was less than 5%.

In order to assess the climatic significance of chemical elements, several published proxy climatic records of DP-2011-02 including dry bulk density (DD), coarse silt and sand fraction of particle size (CSSF) (Zhong et al., 2015a), organic carbon isotopes ($\delta^{13}C_{org}$) (Zhong et al., 2017) and pollen data (Zhong et al., 2015b) were also used in the present study.

4 Results

4.1 Lithology and chronology

Lithology of the core consisted of alternating layers of lake and marsh sediments, incarnating hydrological shifts in this region (Fig. 2). The detailed description of this core profile were recorded was presented in Zhong et al. (2015a). The newly calibrated radiocarbon dates and the age-depth relationship of the core are shown in Table 1 and Fig. 2, respectively. The age-depth model indicated that the bottom age of the core was cal. 15 400 yr B.P..

4.2 Variations in major and trace elements

Variations of the selected elements and element ratios are shown in Figs. 3 and 4, respectively. Prior to 14 500 cal. yr B.P., Al_2O_3, TiO_2 and FeOt (including FeO and Fe_2O_3) and MnO, as well as Rb/Sr ratios exhibited relatively lower values, whereas Ba and Sr displayed increases. From 14 500 to 13 200 cal. yr B.P., the decreasing values of SiO_2/Al_2O_3, MnO/Al_2O_3 and $FeOt/Al_2O_3$ ratios were negatively correlated with Rb/Sr. In contrast, Al_2O_3, TiO_2, FeOt, MnO and Cu exhibited an opposite variation trend compared to Sr and Ba. From 13 200 to 11 000 cal. yr B.P., the values of Sr, MnO/Al_2O_3 and

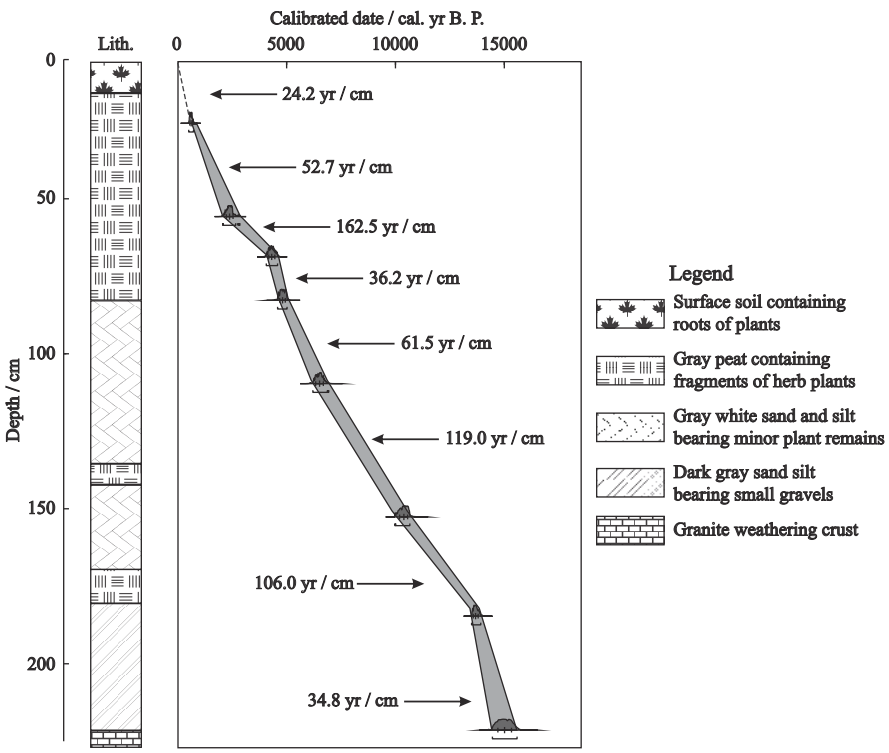

Fig. 2 Lithological structure and the newly constructed age-depth relationship of core DP-2011-02 in Daping swamp. The left part of the map shows the depth and lithology of core DP-2011-02. The gray band in the middle of the graph shows the age-depth relationship on 2σ range. Dark spaced symbols on band represent the marginal posterior distribution considering the depth model and the median of the corrected results. Sedimentation rates between the two adjacent calibrated ages are presented in years per cm (yr/cm). The figure was revised based on Zhong et al. (2015a)

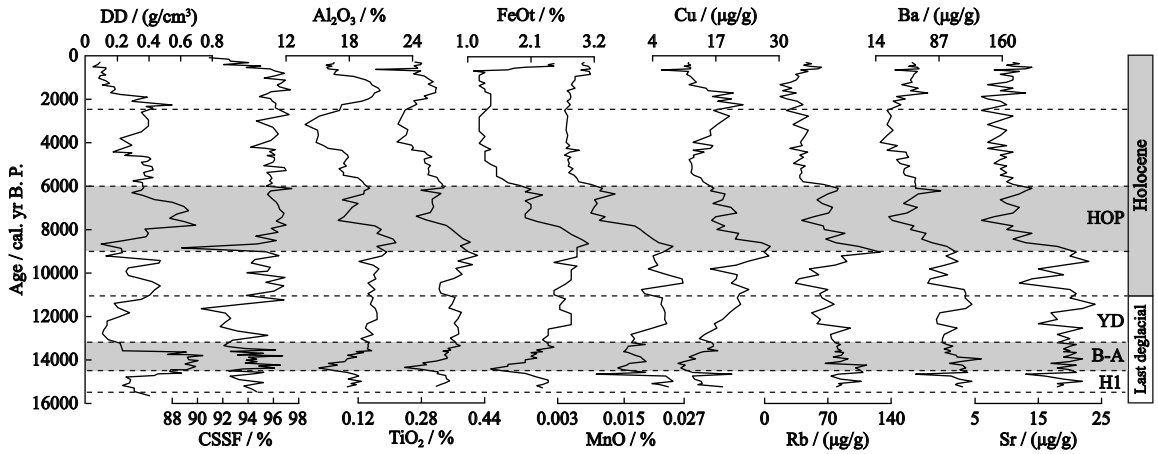

Fig. 3 Variations of major and trace elements contents in core DP-2011-02 of Daping Swamp. The dry bulk density (DD) and coarse silt and sand fraction of particle size (CSSF) data were based on Zhong et al. (2015a; b). H1 and YD refer to the Heinrich event 1 and the Younger Dryas event, respectively. HOP and B-A denote the wet and warm Holocene Optimum period and the Bølling-Allerød events

$FeOt/Al_2O_3$ increased, whereas those of Rb and Rb/Sr decreased apparently. During 11 000−9000 cal. yr B.P., though Ba reached its peak value, it exhibited an overall downward trend during this interval, whereas TiO_2, FeOt, MnO, Cu and Rb displayed an opposite variation trend. Meanwhile, the ratios of $FeOt/Al_2O_3$ and MnO/Al_2O_3 displayed a stepwise decrease. Moreover, Al_2O_3, TiO_2, FeOt, Cu and Rb displayed their maximum values between 9000 and 6000 cal. yr B.P.. The value of the Rb/Sr ratio exhibited a marked increase compared to the preceding period. However, SiO_2/Al_2O_3, MnO/Al_2O_3 and $FeOt/Al_2O_3$ ratios obviously decreased. From 6000 to 2500 yr B.P., the contents of Al_2O_3 and TiO_2 decreased evidently. However, the SiO_2/Al_2O_3 and MnO/Al_2O_3 ratios displayed a gentle increase. During 2500−1000 yr B.P., the contents of Al_2O_3, TiO_2 and Cu increased, whereas the ratios of SiO_2/Al_2O_3, $FeOt/Al_2O_3$ and MnO/Al_2O_3 declined. After 1000 yr B.P., SiO_2/Al_2O_3 and MnO/Al_2O_3, especially $FeOt/Al_2O_3$ increased significantly.

5 Discussion

5.1 Factors controlling the variations of major and trace elements

The accumulation of geochemical elements in lake sediments is closely related to the leaching, transportation and deposition of surface materials in the watershed. Moreover, chemical weathering is an important factor affecting these processes. It is generally accepted that climate plays a major role in controlling the chemical weathering processes, as rainwater is considered to be the first-order control factor initiating chemical weathering and determining the intensity of chemical reactions. Therefore, the changes in intensity of chemical weathering were closely related to the temperature and rainfall conditions of the region. Moreover, wet and warm conditions generally favor highly weathered elements and the chemical composition in sediments due to chemical reactions. Therefore, the weathering intensity was higher than that under dry and cold conditions.

In the core, multiple proxies including $\delta^{13}C_{org}$, DD, CSSF, and pollen data (Zhong et al., 2015a; b; 2017) were used to decipher the changes in hydrological and climatic conditions. Higher $\delta^{13}C_{org}$ and herb pollen concentrations were interpreted to indicate relatively dry and cold conditions (Xue et al., 2014; Rao et al., 2012; 2017; Zhong et al., 2017). The DD and particle grain size could provide more information about the external input of detrital material (Zhou et al., 2004; Xue et al., 2009), with higher DD and CSSF suggesting higher input of clastic materials and relatively coarser materials due to elevated riverine/fluvial, implying a wet and warm condition, and vice versa. Based on these proxy records, our team has constructed the hydrological and climatic history in Daping swamp over the past 15 400 yr (Zhong et al., 2015a; 2017), and several millennial climatic events, such as the Heinrich event 1 (H1) (Heinrich 1988; Stanford et al., 2011), Younger Dryas event (YD), Holocene optimum period (HOP) and the

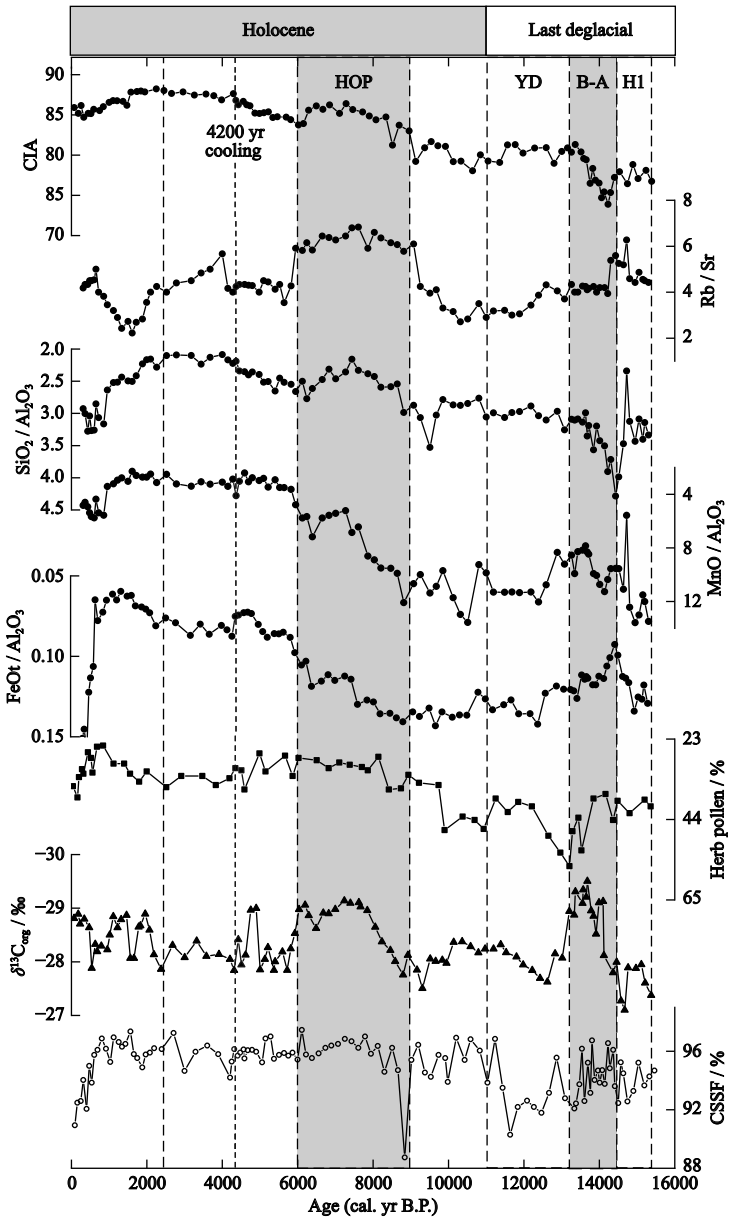

Fig. 4 Variations of multi-proxy records and their possible responses to climatic conditions of core DP-2011-02 in Daping swamp. Data for herb pollen and organic carbon stable isotope ($\delta^{13}C$) were previously published in Zhong et al. (2015b; 2017), The coarse silt and sand fraction of particle size (CSSF) data were based on Zhong et al. (2015a). H1 and YD refer to the Heinrich event 1 and the Younger Dryas event, respectively. The gray bars indicate warm periods: Bølling-Allerød events (B-A) and Holocene Optimum period (HOP). The black dotted line refers to the '4200 yr cooling' event

'4200 yr cooling' event (Wang et al., 2005; Wang, 2011; Pan et al., 2020) were clearly identified. These results indicated that the changes in hydrological conditions in the lake were closely related to the summer monsoon precipitation (Aggarwal et al., 2004; Fan et al., 2017). As shown in Figs. 3 and 4, in comparison with these climatic stages, it can be observed that the decreased contents of mobile and soluble elements (such as Ba and Sr) (Mackereth, 1966; Jin et al., 2001b; Yang et al., 2006; Xu et al., 2010) and increased contents of immobile and resistant elements (for example Al_2O_3, TiO_2, FeOt, MnO, Cu and Rb) (Yancheva et al., 2007; Sun et al., 2010; Wu et al., 2011; Babeesh et al., 2017) corresponded to the warm and humid periods, whereas under dry and cold conditions, they displayed an inverse situation. In this sense, the ratios of Rb/Sr, SiO_2/Al_2O_3, $FeOt/Al_2O_3$ and MnO/Al_2O_3 were used to indicate the changes in the intensity of chemical weath-

ering, with higher Rb/Sr and lower SiO_2/Al_2O_3, $FeOt/Al_2O_3$ and MnO/Al_2O_3 reflecting more intensive chemical weathering, and vice versa. It should be noted that the changes in Daping chemical records exhibited an asynchronous pattern with the Erhai lake in southwest China (Chen et al., 2000; 2005; Shen et al., 2005) and the Daihai lake in the north China (Peng et al., 2005; Jin et al., 2006; Sun et al., 2010), whose Al_2O_3, SiO_2, FeOt and Cu generally displayed lower values during the warm and wet periods, and vice versa. This could be due to the reason that Daping swamp is a small lake located in a closed intermontane basin. Unlike Daihai lake and Erhai lake, the weathered granite residues in the catchment are the dominant sources of sediments, and therefore, the geochemical features of the residues played a role in controlling the chemical characteristics of the sediments.

In the core DP-2011-02, the values of the chemical index of alteration (CIA, $CIA=[(Al_2O_3)/(Al_2O_3+CaO+Na_2O+K_2O)] \times 100$) (Nesbitt and Young 1982; 1989; Fedo et al., 1995), which was related to temperature/precipitation-associated hydrothermal status, lied within the range of 73.9%−88.2% (mean value: 85.3%), indicating a moderate and strong chemical weathering in the past 15 400 yr. As illustrated in Fig. 4, The $\delta^{13}C_{org}$ and herb pollen correlated positively with the values of the SiO_2/Al_2O_3, $FeOt/Al_2O_3$ and MnO/Al_2O_3 ratios. However, the $\delta^{13}C_{org}$ and herb pollen correlated negatively with CIA, CSSF and Rb/Sr, suggesting that the geochemical features of the sediments were deeply impacted by the climate-induced chemical weathering. Meanwhile, the wet and warm conditions would favor more intensive chemical weathering, resulting in enhanced input of weathering residues and leading to depleted mobile and soluble elements in the sediments (Xu et al., 2010; Babeesh et al., 2017). On the contrary, under drier and colder conditions, decreased chemical weathering would favor the enrichment of mobile and soluble elements in the sediments. Additionally, the FeOt and MnO records were often used to indicate redox conditions in the lake body (Haberyan and Hecky 1987; Davison 1993; Wu et al., 2011). Therefore, the increased concentrations of FeOt and MnO suggested intensified oxidizing conditions, implying a shallow-water situation. On the other hand, decreased concentrations of FeOt and MnO indicated increased reducing conditions, suggesting an expansion of lake water body.

As discussed above, it was inferred that the variations of various geochemical records of Daping sediments could serve as indicators of climate-induced chemical weathering. Since the study area was deeply influenced by ASM, the history of chemical weathering as evidenced by the geochemical proxies bore the potential to reconstruct past climatic conditions that was related to the summer monsoon in the past 15 400 yr.

5.2 Variations of chemical weathering intensity in the past 15 400 yr

During the Last Deglacial period (15 400−11 000 yr B. P.), the values of CIA and Rb/Sr ratios displayed lower values in the whole profile (Fig. 4), suggesting relatively weak chemical weathering and an overall relatively dry and cold conditions. Particularly, during the two periods of 15 400−14 500 yr B. P. (H1 event) and 13 200−11 000 yr B. P. (YD event), the CIA and Rb/Sr showed obvious low values, suggesting a decreased chemical weathering. The increased values of $FeOt/Al_2O_3$ and MnO/Al_2O_3 indicated a decline of lake level and intensified oxidation conditions in the water body. The dry conditions were also reflected by increased $\delta^{13}C_{org}$ and herb pollen, as well as decreased CSSF (Fig. 4). Evident increases in the values of CIA and Rb/Sr, as well as decreases in SiO_2/Al_2O_3 ratios between 14 500 and 13 200 yr B. P. suggested an intensified chemical weathering induced by strengthened wet and warm conditions, indicating enhanced summer monsoon. The clear decreases in $\delta^{13}C_{org}$, CSSF and an increase in DD supported this interpretation. This period coincided with the Bølling and Allerød (B-A) warm events. In this period, strengthened humid and warm conditions favored the expansion of lake water body, and the outflow might have carried more insoluble elements (such as Al_2O_3, FeOt and Rb) out of the lake, thus leading to lower CIA but higher SiO_2/Al_2O_3 than those in the YD (Fig. 4).

In the Holocene (11 000−0 yr B. P.) period, various geochemical records displayed drastic variations (Figs. 3 and 4). In the early Holocene (11 000−9 000 yr B.P.) period, significantly increased CIA, Rb/Sr, DD and CSSF, together with slightly declined SiO_2/Al_2O_3 and $FeOt/Al_2O_3$ suggested an enhanced chemical weathering and increased input of terrestrial debris. In particular, the period from 9000 to 6000 yr B. P., which corresponded to the HOP, exhibited significant increase in

CIA and evident decreases in $FeOt/Al_2O_3$ and MnO/Al_2O_3, as well as the maximum Rb/Sr and minimum SiO_2/Al_2O_3, signifying an intensified chemical weathering and strengthened deep-water hypoxic environment. The notable wet and warm conditions were also reflected by evidently decreased values of $\delta^{13}C_{org}$ and herb pollen, as well as increased values of DD and CSSF (Zhong et al., 2017). All the proxy records indicated an abundance of terrestrial plants and enhanced terrigenous debris influx due to the strengthening of EASM.

After 6000 yr B. P., the value of Rb/Sr decreased obviously, whereas the values of $FeOt/Al_2O_3$ and MnO/Al_2O_3 tended to flatten out as compared to the prior stage. Together with higher $\delta^{13}C_{org}$ and lower DD (Fig. 4), the results indicate that the overall climate was relatively dry and cold since 6000 yr B. P.. However, in the period between 6000 and 2500 yr B. P., the CIA displayed relatively higher values, whereas SiO_2/Al_2O_3, $FeOt/Al_2O_3$ and MnO/Al_2O_3 exhibited lower values than those in the HOP. This phenomenon implies the impacts of significant wet and warm conditions in the HOP on the weathered residues. Evident intensified chemical weathering during the HOP resulted in intensive leaching of soluble and mobile elements in the weathered materials. The effects of desilication and allitization would result in significantly Al-enriched and Si-depleted weathered residues, after entering the late Holocene period, these materials were eroded and transported into the lake, and resulted in higher CIA and lower SiO_2/Al_2O_3, $FeOt/Al_2O_3$, and MnO/Al_2O_3 than those in the HOP period. After 2500 yr B.P., the values of SiO_2/Al_2O_3, $FeOt/Al_2O_3$, and MnO/Al_2O_3 decreased slightly, indicating that the climate had shifted towards wet and warm conditions. It was noteworthy that SiO_2/Al_2O_3, $FeOt/Al_2O_3$ and MnO/Al_2O_3 ratios increased significantly after 1000 yr B.P., indicating that the chemical weathering decreased again. Meanwhile, the values of DD and CSSF (Fig. 3) declined evidently, suggesting a climatic shift towards drier and colder conditions.

The millennial H1, B-A and YD events during the Last Deglacial detected from the current geochemical records (Fig. 5a) displayed a consistency with East Asian Summer Monsoon Index (EASMI) (Fig. 5b) (Li et al., 2013), $\delta^{13}C_{org}$ record of Dahu swamp (Fig. 5c) and the the percentage of tropical plants in Huguangyan Maar lake (Leizhou peninsula, South China) (Fig. 5d) (Wang et al., 2016), as well as the stalagmite $\delta^{18}O$ of Dongge cave (Guizhou, Southwest China) (Fig. 5e) (Dykoski et al., 2005) and the Oman Qunf cave (Arabian Peninsula) (Fig. 5f) (Fleitmann et al., 2003) which was considered to be a good indicator of EASM evolution with its lower values indicating strengthened EASM, and *vice versa,* indicating a sensitive response of Daping region to the evolution of Asian monsoon circulation and global climatic changes.

On the orbital scale, the solar radiation may play a role in modulating the climatic changes (Fig. 5g) (Berger and Loutre, 1991; Wei et al., 2020). In this study, the geochemical records indicated that the HOP occurred within the range of 9000−6000 yr B. P. (Fig. 4), the 1000-yr lag of the onset timing of HOP in Daping swamp compared to the Dahu sediments in eastern NLM (Fig. 5c) (Xiao et al., 2007; Wang et al., 2021) as well as other ASM proxy records (Figs. 5b,5d−5f) may be attributed to the 'glacier boundary effect', which was caused by the high latitudes and residual ice on the Tibetan plateau (Wang et al., 2001; Chen et al., 2015; Zhao et al., 2016; Wei et al., 2020).

6 Conclusions

Multiple geochemical records derived from lacustrine sediments of Daping swamp in western Nanling mountains indicated that the accumulation of major and trace elements mainly contributed by inputting weathered residues in the catchment. Changes in the intensity of chemical weathering played a role in controlling the variations of geochemical records. Warmer and wetter climatic conditions would favor stronger chemical weathering, resulting in more soluble and mobile elements (such as Ba and Sr) to be leached and leaving the weathered residues enriched in resistant and insoluble elements (such as Al_2O_3, TiO_2, and Rb). These residues were then eroded and transported to the lake, resulting in the enrichment of insoluble elements in the sediments as evidenced by higher CIA, Rb/Sr and lower SiO_2/Al_2O_3, $FeOt/Al_2O_3$ and MnO/Al_2O_3 ratios. In contrast, under dry and cold conditions, it would exhibit an inverse situation. Since variations in the intensity of chemical weathering were closely related to the changes in climatic conditions, the geochemical records obtained in the current work indirectly reflected that past climatic changes in the study region were associated

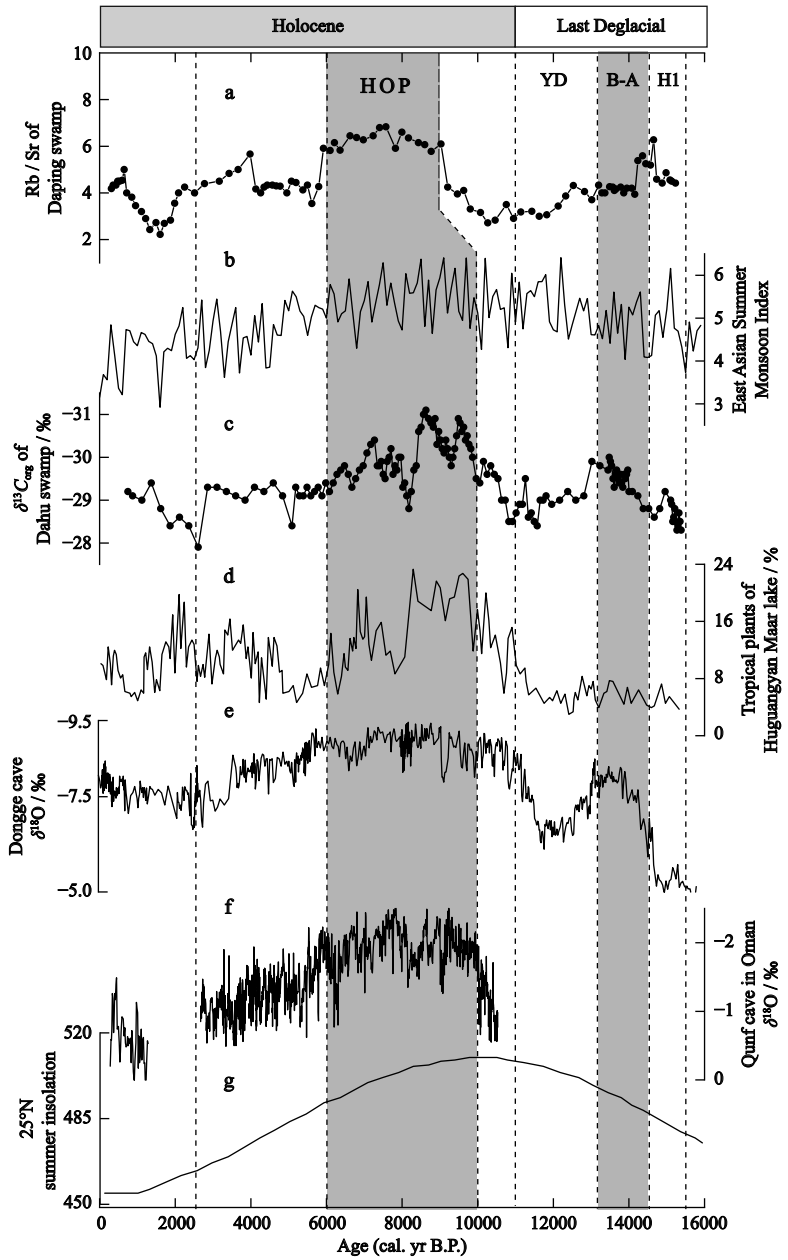

Fig. 5 Comparison of chemical weathering indexes from Daping sediments with various regional climatic records. a: the Rb/Sr ratios from Daping swamp; b: East Asian Summer Monsoon Index (EASMI) (Li et al., 2013); c: $\delta^{13}C_{org}$ record of Dahu swamp (Xue et al., 2009); d: percsentage of tropical plants in Huguangyan Maar lake (Wang et al., 2016); e: stalagmite $\delta^{18}O$ record of Dongge cave (Dykoski et al., 2005); f: stalagmite $\delta^{18}O$ record of Qunf cave in Oman (Fleitmann et al., 2003); g: the summer insolation at 25°N latitude (Berger and Loutre, 1991)

with the Asian summer monsoon. This study provides new data for exploring the response of surface geochemical processes to chemical weathering in the catchment of subalpine lake in South China.

Acknowledgement:

Measurement of conventional ^{14}C dates was carried out at the Key Lab of Western China's Environmental Systems (Ministry of Education of China), Lanzhou University.

References

Aggarwal P K, Fröhlich K, Kulkarni K M et al., 2004. Stable isotope evidence for moisture sources in the Asian summer monsoon under present and past climate regimes. *Geophysical Re-*

search Letters, 31(8): L08203. doi: 10.1029/2004GL019911

Babeesh C, Lone A, Achyuthan H, 2017. Geochemistry of Manasbal lake sediments, Kashmir: weathering, provenance and tectonic setting. *Journal of the Geological Society of India*, 89(5): 563–572. doi: 10.1007/s12594-017-0645-4

Berger A, Loutre M F, 1991. Insolation values for the climate of the last 10 million years. *Quaternary Science Reviews*, 10(4): 297–317. doi: 10.1016/0277-3791(91)90033-Q

Boës X, Rydberg J, Martinez-Cortizas A et al., 2011. Evaluation of conservative lithogenic elements (Ti, Zr, Al, and Rb) to study anthropogenic element enrichments in lake sediments. *Journal of Paleolimnology*, 46(1): 75–87. doi: 10.1007/s10933-011-9515-z

Chen F H, Xu Q H, Chen J H et al., 2015. East Asian summer monsoon precipitation variability since the last deglaciation. *Scientific Reports*, 5(1): 11186. doi: 10.1038/srep11186

Chen J A, Wan G J, Tang D G, 2000. Recent climate changes recorded by sediment grain sizes and isotopes in Erhai Lake. *Progress in Natural Science*, 10(1): 54–61.

Chen J A, Wan G J, Zhang D D et al., 2005. The 'little ice age' recorded by sediment chemistry in Lake Erhai, southwest China. *The Holocene*, 15(6): 925–931. doi: 10.1191/0959683605hl863rr

Davison W, 1993. Iron and manganese in lakes. *Earth-Science Reviews*, 34(2): 119–163. doi: 10.1016/0012-8252(93)90029-7

Degeai J P, Villa V, Chaussé C et al., 2018. Chemical weathering of palaeosols from the Lower Palaeolithic site of Valle Giumentina, central Italy. *Quaternary Science Reviews*, 183: 88–109. doi: 10.1016/j.quascirev.2018.01.014

Dykoski C A, Edwards R L, Cheng H et al., 2005. A high-resolution, absolute-dated Holocene and deglacial Asian monsoon record from Dongge Cave, China. *Earth and Planetary Science Letters*, 233(1-2): 71–86. doi: 10.1016/j.epsl.2005.01.036

Fan J W, Xiao J L, Wen R L et al., 2017. Carbon and nitrogen signatures of sedimentary organic matter from dali lake in inner mongolia: implications for holocene hydrological and ecological variations in the east asian summer monsoon margin. *Quaternary International*, 452: 65–78. doi: 10.1016/j.quaint.2016.09.050

Fedo C M, Wayne Nesbitt H, Young G M, 1995. Unraveling the effects of potassium metasomatism in sedimentary rocks and paleosols, with implications for paleoweathering conditions and provenance. *Geology*, 23(10): 921–924. doi: 10.1130/0091-7613(1995)023<0921:UTEOPM>2.3.CO;2

Fleitmann D, Burns S J, Mudelsee M et al., 2003. Holocene forcing of the Indian monsoon recorded in a stalagmite from southern Oman. *Science*, 300(5626): 1737–1739. doi: 10.1126/science.1083130

Gao Y X, Xu S Y, Guo Q Y et al. , 1962. Monsoon region and regional climate in China. In: Gao Y et al. (ed). *Some Problems of East Asian Monsoon*. Beijing: Science Press, 49 –63. (in Chinese)

Gislason S R, Oelkers E H, Eiriksdottir E S et al., 2009. Direct evidence of the feedback between climate and weathering. *Earth and Planetary Science Letters*, 277(1-2): 213–222. doi: 10.1016/j.epsl.2008.10.018

Haberyan K A, Hecky R E, 1987. The late Pleistocene and Holocene stratigraphy and paleolimnology of Lakes Kivu and Tanganyika. *Palaeogeography, Palaeoclimatology, Palaeoecology*, 61: 169–197. doi: 10.1016/0031-0182(87)90048-4

Hartmann J, Moosdorf N, 2011. Chemical weathering rates of silicate-dominated lithological classes and associated liberation rates of phosphorus on the Japanese Archipelago—Implications for global scale analysis. *Chemical Geology*, 287(3-4): 125–157. doi: 10.1016/j.chemgeo.2010.12.004

Heinrich H, 1988. Origin and consequences of cyclic ice rafting in the northeast Atlantic Ocean during the past 130 000 years. *Quaternary Research*, 29(2): 142–152. doi: 10.1016/0033-5894(88)90057-9

Jin Z D, Wang S M, Shen J et al., 2001a. Weak chemical weathering during the Little Ice Age recorded by lake sediments. *Science in China Series D: Earth Sciences*, 44(7): 652–658. doi: 10.1007/BF02875338

Jin Z D, Wang S M, Shen J et al., 2001b. Chemical weathering since the Little Ice Age recorded in lake sediments: a high-resolution proxy of past climate. *Earth Surface Processes and Landforms*, 26(7): 775–782. doi: 10.1002/esp.224

Jin Z D, Li F C, Cao J J et al., 2006. Geochemistry of Daihai Lake sediments, Inner Mongolia, North China: implications for provenance, sedimentary sorting, and catchment weathering. *Geomorphology*, 80(3-4): 147–163. doi: 10.1016/j.geomorph.2006.02.006

Li C, Yang S Y, 2010. Is chemical index of alteration (CIA) a reliable proxy for chemical weathering in global drainage basins? *American Journal of Science*, 310(2): 111–127. doi: 10.2475/02.2010.03

Li J R, Liu S F, Shi X F et al., 2021. Applicability and variability of chemical weathering indicators and their monsoon-controlled mechanisms in the Bay of Bengal. *Frontiers in Earth Science*, 9: 633713. doi: 10.3389/feart.2021.633713

Li X Z, Liu X D, Qiu L J et al., 2013. Transient simulation of orbital-scale precipitation variation in monsoonal East Asia and arid central Asia during the last 150 ka. *Journal of Geophysical Research:Atmospheres*, 118(14): 7481–7488. doi: 10.1002/jgrd.50611

Liu J, Zhong J, Chen S et al., 2021. Hydrological and biogeochemical controls on temporal variations of dissolved carbon and solutes in a karst river, South China. *Environmental Sciences Europe*, 33(1): 53. doi: 10.1186/s12302-021-00495-x

Liu S F, Li J R, Zhang H et al., 2020. Complex response of weathering intensity registered in the Andaman Sea sediments to the Indian Summer Monsoon over the last 40 kyr. *Marine Geology*, 426: 106206. doi: 10.1016/j.margeo.2020.106206

Machlus M L, Ramezani J, Bowring S A et al., 2015. A strategy for cross-calibrating U-Pb chronology and astrochronology of sedimentary sequences: an example from the Green River Formation, Wyoming, USA. *Earth and Planetary Science Letters*, 413: 70–78. doi: 10.1016/j.epsl.2014.12.009

Mackereth F J H, 1966. Some chemical observations on post-glacial lake sediments. *Philosophical Transactions of the Royal Society of London. Series B, Biological Sciences*, 250(765): 165–213. doi: 10.2307/2416701

Miriyala P, Sukumaran N P, Nath B N et al., 2017. Increased chemical weathering during the deglacial to mid-Holocene summer monsoon intensification. *Scientific Reports*, 7(1): 44310. doi: 10.1038/srep44310

Nesbitt H W, Young G M, 1982. Early proterozoic climates and plate motions inferred from major element chemistry of lutites. *Nature*, 299(5885): 715–717. doi: 10.1038/299715a0

Nesbitt H W, Young G M, 1989. Formation and diagenesis of weathering profiles. *The Journal of Geology*, 97(2): 129–147. doi: 10.1086/629290

Pan J Y, Zhong W, Wei Z Q et al., 2020. A 15, 400-year record of natural and anthropogenic input of mercury (Hg) in a subalpine lacustrine sediment succession from the western Nanling Mountains, South China. *Environmental Science and Pollution Research*, 27(16): 20478–20489. doi: 10.1007/s11356-020-08421-z

Peng Y J, Xiao J L, Nakamura T et al., 2005. Holocene East Asian monsoonal precipitation pattern revealed by grain-size distribution of core sediments of Daihai Lake in Inner Mongolia of north-central China. *Earth and Planetary Science Letters*, 233(3-4): 467–479. doi: 10.1016/j.epsl.2005.02.022

Qian W H, Lin X, Zhu Y F et al., 2007. Climatic regime shift and decadal anomalous events in China. *Climatic Change*, 84(2): 167–189. doi: 10.1007/s10584-006-9234-z

Rao Z G, Chen F H, Zhang X et al., 2012. Spatial and temporal variations of C_3/C_4 relative abundance in global terrestrial ecosystem since the Last Glacial and its possible driving mechanisms. *Chinese Science Bulletin*, 57(31): 4024–4035. doi: 10.1007/s11434-012-5233-9

Rao Z G, Guo W K, Cao J T et al., 2017. Relationship between the stable carbon isotopic composition of modern plants and surface soils and climate: a global review. *Earth-Science Reviews*, 165: 110–119. doi: 10.1016/j.earscirev.2016.12.007

Reimer P J, Austin W E N, Bard E et al., 2020. The IntCal20 Northern Hemisphere radiocarbon age calibration curve (0–55 cal kBP). *Radiocarbon*, 62(4): 725–757. doi: 10.1017/RDC.2020.41

Shen J, Yang L Y, Yang X D et al., 2005. Lake sediment records on climate change and human activities since the Holocene in Erhai catchment, Yunnan Province, China. *Science in China Series D:Earth Sciences*, 48(3): 353–363. doi: 10.1360/03yd0118

Stanford J D, Rohling E J, Bacon S et al., 2011. A new concept for the paleoceanographic evolution of Heinrich event 1 in the North Atlantic. *Quaternary Science Reviews*, 30(9-10): 1047–1066. doi: 10.1016/j.quascirev.2011.02.003

Sun Q L, Wang S M, Zhou J et al., 2010. Sediment geochemistry of Lake Daihai, north-central China: implications for catchment weathering and climate change during the Holocene. *Journal of Paleolimnology*, 43(1): 75–87. doi: 10.1007/s10933-009-9315-x

Wang Chunlong, Liu Sha, Wu Jing et al., 2013. Ore-forming element distribution around the southwestern domain of the Miaoershan-Yuechengling complex in the northeastern Guangxi and its geological implication. *Geochimica*, 42(5): 405–413. (in Chinese)

Wang P, Du Y S, Yu W C et al., 2020. The chemical index of alteration (CIA) as a proxy for climate change during glacial-interglacial transitions in Earth history. *Earth-Science Reviews*, 201: 103032. doi: 10.1016/j.earscirev.2019.103032

Wang Shaowu, 2011. *The Holocene Climate Change*. Beijing: China Meteorological Press, 114–116. (in Chinese)

Wang X J, Zhong W, Li T H et al., 2021. A 16.2-kyr lacustrine sediment record of mercury deposition in Dahu Swamp, eastern Nanling Mountains, southern China: analysis of implications for climatic changes. *Quaternary International*, 592: 12–21. doi: 10.1016/j.quaint.2021.04.013

Wang X S, Chu G Q, Sheng M et al., 2016. Millennial-scale Asian summer monsoon variations in South China since the last deglaciation. *Earth and Planetary Science Letters*, 451: 22–30. doi: 10.1016/j.epsl.2016.07.006

Wang Y J, Cheng H, Edwards R L et al., 2001. A high-resolution absolute-dated late Pleistocene monsoon record from Hulu Cave, China. *Science*, 294(5550): 2345–2348. doi: 10.1126/science.1064618

Wang Y J, Cheng H, Edwards R L et al., 2005. The Holocene Asian monsoon: links to solar changes and North Atlantic climate. *Science*, 308(5723): 854–857. doi: 10.1126/science.1106296

Wei Z Q, Zhong W, Xue J B et al., 2020. Late Quaternary East Asian summer monsoon variability deduced from lacustrine mineral magnetic records of Dahu Swamp, southern China. *Paleoceanography and Paleoclimatology*, 35(2): e2019PA003796. doi: 10.1029/2019PA003796

White A F, Blum A E, 1995. Effects of climate on chemical weathering in watersheds. *Geochimica et Cosmochimica Acta*, 59(9): 1729–1747. doi: 10.1016/0016-7037(95)00078-E

White A F, Brantley S L, 2003. The effect of time on the weathering of silicate minerals: why do weathering rates differ in the laboratory and field? *Chemical Geology*, 202(3-4): 479–506. doi: 10.1016/j.chemgeo.2003.03.001

Wu Xudong, Shen Ji, Wang Yong, 2011. The Holocene climate linkage between low latitude area and North Atlantic: case study on element and element ratios of Huguangyan Maar lake. *Acta Sedimentologica Sinica*, 29(5): 926–934. (in Chinese)

Wu Zhengyi, 1980. *Vegetation of China*. Beijing: Science Press, 825 (in Chinese)

Xiao J Y, Lü H B, Zhou W J et al., 2007. Evolution of vegetation and climate since the last glacial maximum recorded at Dahu peat site, South China. *Science in China Series D:Earth Sciences*, 50(8): 1209–1217. doi: 10.1007/s11430-007-0068-y

Xu H, Liu B, Wu F, 2010. Spatial and temporal variations of Rb/Sr ratios of the bulk surface sediments in Lake Qinghai. *Geochemical Transactions*, 11(1): 3. doi: 10.1186/1467-4866-

11-3

Xue Jibin, Zhong Wei, Zheng Yanming et al., 2009. A new high-resolution Late Glacial-Holocene climatic record from eastern Nanling Mountains in South China. *Chinese Geographical Science*, 19(3): 274–282. doi: 10.1007/s11769-009-0274-y

Xue J B, Zhong W, Cao J Y, 2014. Changes in C_3 and C_4 plant abundances reflect climate changes from 41, 000 to 10, 000 yr ago in northern Leizhou Peninsula, South China. *Palaeogeography, Palaeoclimatology, Palaeoecology*, 396: 173–182. doi: 10.1016/j.palaeo.2014.01.003

Yancheva G, Nowaczyk N R, Mingram J et al., 2007. Influence of the intertropical convergence zone on the East Asian monsoon. *Nature*, 445(7123): 74–77. doi: 10.1038/nature05431

Yang S Y, Li C X, Cai J G, 2006. Geochemical compositions of core sediments in eastern China: implication for Late Cenozoic palaeoenvironmental changes. *Palaeogeography, Palaeoclimatology, Palaeoecology*, 229(4): 287–302. doi: 10.1016/j.palaeo.2005.06.026

Yeloff D, Bennett K D, Blaauw M et al., 2006. High precision ^{14}C dating of Holocene peat deposits: a comparison of Bayesian calibration and wiggle-matching approaches. *Quaternary Geochronology*, 1(3): 222–235. doi: 10.1016/j.quageo.2006.08.003

Zhao K, Wang Y J, Edwards R L et al., 2016. Contribution of ENSO variability to the East Asian summer monsoon in the late Holocene. *Palaeogeography, Palaeoclimatology, Palaeoecology*, 449: 510–519. doi: 10.1016/j.palaeo.2016.02.044

Zhong W, Cao J Y, Xue J B et al., 2015a. A 15, 400-year record of climate variation from a subalpine lacustrine sedimentary sequence in the western Nanling Mountains in South China. *Quaternary Research*, 84(2): 246–254. doi: 10.1016/j.yqres.2015.06.002

Zhong W, Cao J Y, Xue J B et al., 2015b. Last deglacial and Holocene vegetation evolution and climate variability in the subalpine western Nanling Mountains in South China. *The Holocene*, 25(8): 1330–1340. doi: 10.1177/0959683615584206

Zhong W, Wei Z Q, Chen Y et al., 2017. A 15.4-ka paleoclimate record inferred from $\delta^{13}C$ and $\delta^{15}N$ of organic matter in sediments from the sub-alpine Daping Swamp, western Nanling Mountains, South China. *Journal of Paleolimnology*, 57(2): 127–139. doi: 10.1007/s10933-016-9935-x

Zhou W J, Yu X F, Jull A J T et al., 2004. High-resolution evidence from southern China of an early holocene optimum and a mid-Holocene dry event during the past 18, 000 years. *Quaternary Research*, 62(1): 39–48. doi: 10.1016/j.yqres.2004.05.004

Zhu J C, Wang R C, Zhang P H et al., 2009. Zircon U-Pb geochronological framework of Qitianling granite batholith, middle part of Nanling Range, South China. *Science in China Series D: Earth Sciences*, 52(9): 1279–1294. doi: 10.1007/s11430-009-0154-4